EurJIC
European Journal of Inorganic Chemistry

Research Article
doi.org/10.1002/ejic.202500275

Chemistry Europe
European Chemical Societies Publishing

www.eurjic.org

Coordination Chemistry of Copper and Nickel with Xenon Difluoride and the Hexafluororuthenate(V) Anion: Synthesis and Structural Studies

Tomaž Mržljak, Evgeny Goreshnik, Gašper Tavčar, and Melita Tramšek*

In the photochemical reactions between MF_2 (M = Cu, Ni), Ru, and F_2 in anhydrous HF, $Cu(RuF_6)_2$, and $Ni(RuF_6)_2$ are formed. Only crystals of $Cu(RuF_6)_2$ are obtained during the crystallization of the powdered products. $Cu(RuF_6)_2$ crystallizes in the triclinic space group $P\bar{1}$. The Cu atoms are coordinated by six F atoms, which are shared with octahedral RuF_6 units. Together, they form slabs that are interconnected by van der Waals forces. In the reactions between $M(RuF_6)_2$ (M = Cu, Ni) and $2XeF_2$ (1:2 molar ratio), $[Cu(XeF_2)_2](RuF_6)_2$ and $[Ni(XeF_2)_2](RuF_6)_2$ are formed. They both crystallize in the monoclinic space group $P2_1/c$. The metal center is coordinated by six F atoms. Two F atoms are provided by two nonbridging XeF_2 molecules, while the remaining four originate from four bridging $[RuF_6]^-$ anions. In the reactions between $M(RuF_6)_2$ (M = Cu, Ni) and an excess of XeF_2, $[Cu(XeF_2)_6](RuF_6)_2$ and $[Ni(XeF_2)_6](RuF_6)_2$ are formed. They are not isostructural, as the first crystallizes in the triclinic space group $P\bar{1}$, while the second crystallizes in the trigonal space group $R\bar{3}$. In both cases, homoleptic cations $[M(XeF_2)_6]^{2+}$ are present, with the metal center coordinated by six nonbridging XeF_2 molecules, while the $[RuF_6]^-$ anions are discrete.

1. Introduction

Noble gases were long considered to be unreactive, until Neil Bartlett synthesized the first noble gas compound, $XePtF_6$, in 1962.[1] Within less than a year, a large number of noble gas compounds had been prepared and characterized, including XeF_2.[2] XeF_2 is one of the simplest noble gas compounds to handle, and therefore, its chemistry is among the most extensively studied. It is a good oxidizing and fluorinating agent, but it can also act as a moderately strong Lewis base and coordinate to metal ions.[3] The first compound with XeF_2 as a ligand to the metal center was $[Ag(XeF_2)_2]AsF_6$.[4] Syntheses of various new coordination compounds with the general formula $[M^{x+}(XeF_2)_n](AF_6)_x$ followed,[5] where "M" is the metal center (e.g., Ag, Li, alkaline earth metals (Mg–Ba), Ni,[6] Cu,[7,8] Zn, Cd, Pb, some lanthanide metals, and Bi[9]), "*x*" its oxidation state, "*n*" the number of coordinated XeF_2 molecules, and $[AF_6]^-$ a weak Lewis base formed in the reaction between MF_2 and a strong Lewis acid AF_5 (e.g., AsF_5, SbF_5, BiF_5).[3,5] By combining different metal centers and Lewis acids, the resulting compounds exhibit different structural types: molecular structures, dimeric structures, chain structures, double chain structures, layer structures, double layer structures, 3D networks, or structures with homoleptically coordinated centers and discrete AF_6 units. Characterization of these compounds has mostly been done using Raman spectroscopy and single-crystal X-ray diffraction. The characteristic Raman bands of coordinated XeF_2 are located between 500 and 600 cm^{-1}: the bands in the 500–535 cm^{-1} range belong to the stretching vibrations of Xe−F(M) (bridging F atom) bonds in bridging XeF_2, that connects two metal centers, while the bands in the range 544–584 cm^{-1} usually belong to the stretching vibrations of Xe−F bonds (nonbridging F atom) in nonbridging XeF_2. The synthesis is usually carried out in anhydrous HF (aHF). One of the synthetic routes, which is also used in this work, is the reaction between $M(AF_6)_2$ and XeF_2.[3] In this work, the starting compound $M(RuF_6)_2$ (M = Cu, Ni) was synthesized by a photochemical reaction between MF_2, F_2, and Ru. So far, several compounds of the type $M_x(Ru^VF_6)_y$ have been synthesized and characterized, e.g., $KRuF_6$,[10] $CsRuF_6$,[10] $LiRuF_6$,[11] $RbRuF_6$[12] (and $AgFRuF_6$[13]). However, $Cu(RuF_6)_2$ is the first structurally characterized salt of the type $M^{II}(A^VF_6)_2$ with a $[RuF_6]^-$ anion. $Ni(RuF_6)_2$ was also synthesized, but the attempts to grow single crystals were unsuccessful; however, a Raman spectrum of the powdered product was obtained.

Nickel as a suitable metal for the preparation of coordination compounds with XeF_2 was perceived only recently. So far, the only known coordination compound with Ni as the metal center has been $[Ni(XeF_2)_2](IrF_6)_2$, whose crystals were unexpectedly obtained.[6] This work presents the crystal structures of $[Ni(XeF_2)_2](RuF_6)_2$ and $[Ni(XeF_2)_6](RuF_6)_2$, as a result of a systematic study of such compounds with Ni as the metal center. The article

T. Mržljak, E. Goreshnik, G. Tavčar, M. Tramšek
Department of Inorganic Chemistry and Technology
Jožef Stefan Institute
Jamova cesta 39, 1000 Ljubljana, Slovenia
E-mail: melita.tramsek@ijs.si

T. Mržljak, E. Goreshnik, G. Tavčar, M. Tramšek
Jožef Stefan International Postgraduate School
Jamova cesta 39, 1000 Ljubljana, Slovenia

Supporting information for this article is available on the WWW under https://doi.org/10.1002/ejic.202500275

Research Article
doi.org/10.1002/ejic.202500275

also presents the syntheses and crystal structures of $[Cu(XeF_2)_n](RuF_6)_2$ ($n = 2, 6$) compounds. Before this report, $[Ba(XeF_2)_5](RuF_6)_2$ was the only known coordination compound with XeF_2 ligand and $[RuF_6]^-$ as the counterion.[14]

2. Results and Discussion

2.1. Crystal Structure of $Cu(RuF_6)_2$ and Raman Characterization of $M(RuF_6)_2$ (M = Cu, Ni)

$M(RuF_6)_2$ (M = Cu, Ni) were synthesized under photochemical reaction conditions (ultraviolet light (UV)) (Equation (1)). Further information on photochemical reactions in which UV light is used for the dissociation of F_2 molecules can be found in the literature.[15]

$$MF_2 + 2Ru + 5F_2 \xrightarrow[298K]{aHF,\ UV} M(RuF_6)_2 \quad (1)$$

We have selected a salt in which the anion ($[AF_6]^-$), Lewis base, is sufficiently large and its negative charge is delocalized over multiple F atoms. This makes the anion only weakly coordinated to the metal cation, allowing it to be replaced by another ligand (e. g. XeF_2, AsF_3, HF, …) within the coordination sphere. In general, the stronger the Lewis acid AF_5, the weaker is its corresponding Lewis base $[AF_6]^-$. Weaker Lewis base coordinates less strongly to a metal center. One approach to classify the strength of Lewis acids is by using fluoride ion affinity (FIA). Based on the computations, RuF_5 is stronger Lewis acid (FIA = 517 kJ mol^{-1}) than some Lewis acids that have already been used in the synthesis of coordination compounds of the type $[M^{x+}(XeF_2)_n](AF_6)_x$, such as SbF_5 (FIA = 501 kJ mol^{-1}), AsF_5 (FIA = 430 kJ mol^{-1}), and PF_5 (FIA = 398 kJ mol^{-1}).[16,17] From this, it follows that $[RuF_6]^-$ is a relatively weak Lewis base and could therefore be easily replaced by XeF_2 in the coordination sphere. Further information on the replacement of weakly coordinating anions by the XeF_2 ligand in the coordination sphere can be found in the literature.[3,5,18,19]

2.1.1. Crystal Structure

Crystallization from a solution of $M(RuF_6)_2$ in aHF yielded colorless plate-like crystals for M = Cu, whereas the crystallization in the case of M = Ni was unsuccessful. The crystal data and refinement results for $Cu(RuF_6)_2$ are given in **Table 1**.

Salts of the general formula $M^{II}(A^{V}F_6)_2$ (M = Mg, d-block metal, A = Nb, Ta, Au, As, Sb, Bi), including $Cu(RuF_6)_2$ (and $Ni(RuF_6)_2$), can be divided into seven groups based on their crystal structure (Types I–VII).[20] The crystal structure of $Cu(RuF_6)_2$ belongs to Type I. It crystallizes in the triclinic space group $P\bar{1}$. The first reported example of the structural Type I was $Ag(SbF_6)_2$,[21] followed by a series of reports of compounds with the crystal structure of the same type, including $M(SbF_6)_2$ (M = Mn,[22] Cu,[23] Pd,[23] Au[24]), $Pd(AsF_6)_2$,[25] $Ag(AF_6)_2$ (A = Ta,[26] Bi[13]) and $Cu(AuF_6)_2$.[20] The key feature of the crystal structures in Type I is the presence of layers of MF_6 and AF_6 octahedral units (**Figure 1**) connected by shared F atoms. In each individual

Table 1. Crystal data and structure refinement for $Cu(RuF_6)_2$.

Parameter	Value
Fw [g mol^{-1}]	493.68
T [K]	150
Crystal system	Triclinic
Space group	$P\bar{1}$
a [Å]	4.9969(2)
b [Å]	5.2975(2)
c [Å]	8.6399(3)
α [°]	75.610(3)
β [°]	88.967(3)
γ [°]	62.831(4)
V [Å^3]	195.88(1)
Z	1
D_{calcd} [g cm^{-3}]	4.185
λ [Å]	0.71073
μ [mm^{-1}]	6.677
GOF[a)]	1.074
R_1[b)]	0.0201
wR_2[c)]	0.0498

[a)]GOF = $\left[\sum w(F_o^2 - F_c^2)^2/(N_o - N_p)\right]^{1/2}$, where N_o = no. of refines and N_p = no. of refined parameters. [b)]$R_1 = \sum||F_o| - |F_c||/\sum|F_o|$. [c)]$wR_2 = [\sum w(F_o^2 - F_c^2)^2/\sum(w(F_o^2)^2]^{1/2}$.

MF_6 layer, M^{2+} cations lie in the same plane. They are connected by AF_6 units, which lie above and below them, forming slabs that are connected only by van der Waals forces (**Figure 2**).[20]

The CuF_6 octahedron is strongly elongated (**Table 2**). Cu−F4 bonds are longer (2.183(2) Å) than other Cu−F bonds (0.243(2) Å longer compared to Cu−F5 and 0.242(2) Å longer compared to Cu−F6). An ideal octahedron would belong to the O_h symmetry, but due to the elongation, the symmetry is reduced to D_{4h}. The cause of this phenomenon, known as the Jahn–Teller effect (JT effect) or Jahn–Teller distortion, is in the d^9 configuration of the Cu^{2+} ion, which is the most studied of all transition metal ions.[27] The JT effect is characteristic of a nonlinear system in a degenerate energy state, where it spontaneously distorts. This distortion lowers the overall energy of the system by splitting the energy levels and thus removing the degeneracy. The result is a more energetically favorable state. The distortion can lead either to a compressed or an elongated octahedron.[28] In the case of the d^9 configuration, two degenerate states are possible—the unpaired electron can occupy either the d_{z^2} or the $d_{x^2-y^2}$ orbital. In CuF_6 octahedron, the unpaired electron occupies the $d_{x^2-y^2}$ orbital (the HOMO orbital), which results in elongation. The energy of the d_{z^2} orbital, which is occupied by two electrons, is lowered (elongation of the bonds along the z-axis), while the energy of the $d_{x^2-y^2}$ orbital with a single electron increases.[29] The same effect is observed in the other two Cu salts of Type I, $Cu(AuF_6)_2$ and $Cu(SbF_6)_2$, as seen by the comparison of the bond lengths of the CuF_6 octahedra in Table 2.[20]

The JT effect is not observed in all salts of Type I, such as $Mn(SbF_6)_2$, $Pd(AsF_6)_2$, and $Pd(SbF_6)_2$. Mn^{2+} has a d^5 configuration,

Research Article
doi.org/10.1002/ejic.202500275

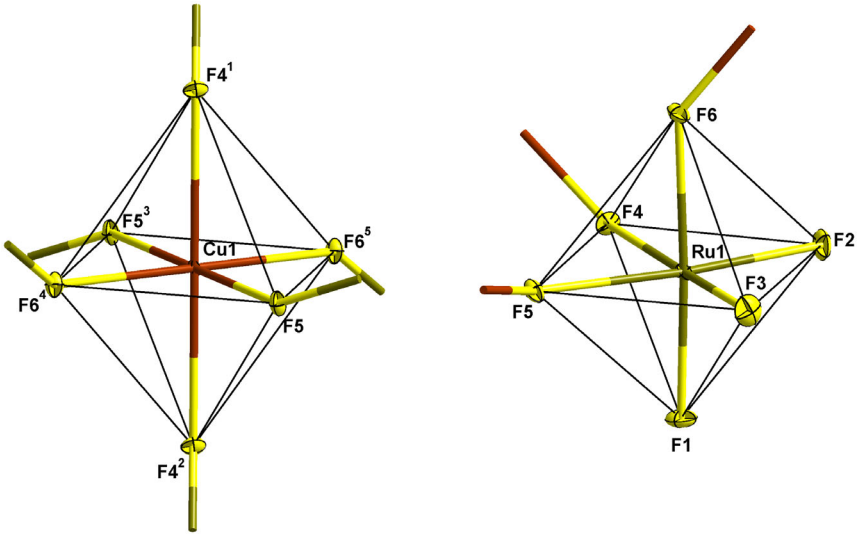

Figure 1. Coordination of Cu (left) and Ru (right) atoms in the crystal structure of $Cu(RuF_6)_2$. Both coordination polyhedra are octahedral, where F atoms act as ligands. Thermal ellipsoids are drawn at a 50% probability level. Symmetry operations used for generation of equivalent atoms: $^{1}-1+x, 1+y, +z$; $^{2}2-x, -y, 1-z$; $^{3}1-x, 1-y, 1-z$; $^{4}+x, 1+y, +z$; $^{5}1-x, -y, 1-z$.

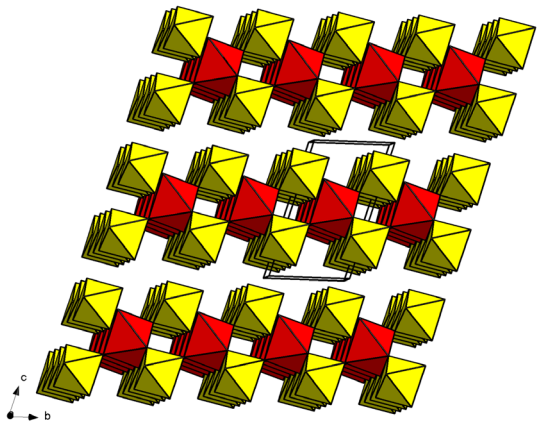

Figure 2. Packing in the crystal structure of $Cu(RuF_6)_2$. The red octahedra represent CuF_6 units, while the yellow octahedra represent RuF_6 units. The unit cell is also shown.

Table 2. A comparison of the bond lengths (Å) in the CuF_6 octahedral units of $Cu(RuF_6)_2$, $Cu(AuF_6)_2$ and $Cu(SbF_6)_2$.

$Cu(RuF_6)_2$	$Cu(AuF_6)_2$[a)]	$Cu(SbF_6)_2$[b)]
2 × 2.183(2)	2 × 2.142(8)	2 × 2.198(2)
2 × 1.941(2)	2 × 1.962(9)	2 × 1.960(2)
2 × 1.940(2)	2 × 1.938(8)	2 × 1.934(2)

[a)]Ref. [20]. [b)]Ref. [23].

while Pd^{2+} has a d^8 configuration.[22,23,25] Not all electron configurations are JT active. For example, the high-spin d^5 and the d^8 configuration are considered JT inactive. Moreover, the JT effect may not be observable even in potentially active systems if the distortion involves the splitting of the degenerate t_{2g} orbitals, which typically has a minimal or negligible impact on the metal−ligand (M—L) bonding.[28]

The $[RuF_6]^-$ octahedron is also distorted, as there are two types of F ligands, three bridging F atoms, which are shared with Cu atom (F4, F5, and F6), and three nonbridging F atoms (F1, F2, and F3), as shown in Figure 1. The Ru−F bonds are shorter than Ru−F(M) bonds—the same trend is observed for the bond lengths in anions $[AF_6]^-$ of the isotypic crystal structures of $Cu(AuF_6)_2$ and $Cu(SbF_6)_2$ (**Table 3**). The bonds in the $[RuF_6]^-$ octahedron are shorter than those in the $[AuF_6]^-$ and $[SbF_6]^-$ octahedra, both for nonbridging (A—F) and bridging (A—F(M)) F atoms.[20,23]

Since the Raman spectrum of the powdered product of $Ni(RuF_6)_2$ (**Figure 3**b) is very similar to the Raman spectrum of $Cu(RuF_6)_2$ (Figure 3a), this compound could also belong to the group of salts with a crystal structure of the Type I. Contrary to expectations, the Ni salt $Ni(SbF_6)_2$, whose crystal structure is also unknown, is classified based on vibrational analysis as a member of the group of salts of the Type II, where MF_6 and AF_6 units form a three-dimensional framework. This is different for Cu salts, where both $Cu(RuF_6)_2$ and $Cu(SbF_6)_2$ belong to Type I.[20,21,23]

Table 3. A comparison of the bond lengths (Å) in the $[AF_6]^-$ anions of $Cu(RuF_6)_2$, $Cu(AuF_6)_2$ and $Cu(SbF_6)_2$.

Bonding atoms	$Cu(RuF_6)_2$	$Cu(AuF_6)_2$[a)]	$Cu(SbF_6)_2$[b)]
A—F	1.800(2)	1.865(9)	1.831(2)
	1.804(2)	1.868(8)	1.841(2)
	1.815(2)	1.868(9)	1.846(2)
A—F(M)	1.882(2)	1.934(9)	1.890(2)
	1.937(2)	1.953(8)	1.951(2)
	1.940(2)	1.947(9)	1.965(2)

[a)]Ref. [20]. [b)]Ref. [23].

Research Article
doi.org/10.1002/ejic.202500275

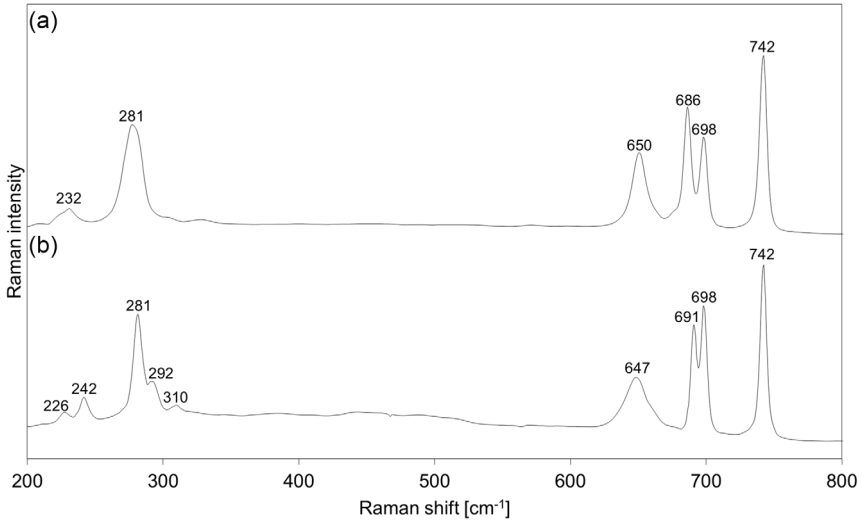

Figure 3. Raman spectra of the powdered products of a) $Cu(RuF_6)_2$ and b) $Ni(RuF_6)_2$. Raman spectra were recorded through a quartz capillary.

2.1.2. Raman Characterization

The Raman spectra of the powdered products of $Cu(RuF_6)_2$ and $Ni(RuF_6)_2$ show bands at similar wavenumber values (Figure 3a,b). The Raman spectrum of the $Cu(RuF_6)_2$ crystal (Figure S1, Supporting Information) matches the Raman spectrum of the powdered product.

For octahedral species ($[RuF_6]^-$) with O_h symmetry, six normal vibrational modes are characteristic. Among these, ν_1, ν_2, and ν_5 are Raman active.[30] As can be seen from the Raman spectrum of both compounds, more than three bands are present. Due to the symmetry lowering and strong cation−anion interactions in the crystal structure, some vibrations that are inactive in O_h symmetry may become active, and there may also be splitting of some vibrations.[31] The Raman spectra of $Cu(RuF_6)_2$ and $Ni(RuF_6)_2$ are comparable to the Raman spectra of the compounds $M(SbF_6)_2$ (M = Cr, Mn, Fe, Cu, Pd, Ag), as all show several intense bands in the wavenumber range of ≈640 to 740 cm^{-1}. This is consistent with the fact that the crystal structures of these antimonates (except for M = Cr, Fe, where the crystal structures are unknown) are isotypic to the crystal structure of $Cu(RuF_6)_2$ and possibly also to the crystal structure of $Ni(RuF_6)_2$. The differences between the spectra of antimonates and ruthenates is in the position of the band at the highest wavenumber (for antimonates, it is between 718 ($Ag(SbF_6)_2$) and 726 cm^{-1} ($Cu(SbF_6)_2$), while for ruthenates, it is at 742 cm^{-1}) and in the position of the band with the highest intensity (for antimonates, it is the band in the range between 643 ($Mn(SbF_6)_2$) and 654 cm^{-1} ($Cu(SbF_6)_2$), while for ruthenates, it is the band at the highest wavenumber (742 cm^{-1}).[32] The Raman spectrum of $Cu(AuF_6)_2$, whose crystal structure is also isotypic to the crystal structures of the mentioned antimonates and ruthenates, is less similar to the Raman spectra of $Cu(RuF_6)_2$ and $Ni(RuF_6)_2$. The bands appear at lower wavenumbers, with the highest frequency band located at 667 cm^{-1} and the most intense band at 603 cm^{-1}.[20]

2.2. Crystal Structure and Raman Characterization of $[M(XeF_2)_2](RuF_6)_2$ (M = Cu, Ni)

$Cu(RuF_6)_2$ and $Ni(RuF_6)_2$ were together with XeF_2 reactants for the synthesis of compounds of the type $[M(XeF_2)_n](RuF_6)_2$.

2.2.1. Crystal Structure

Crystals of $[Cu(XeF_2)_2](RuF_6)_2$ and $[Ni(XeF_2)_2](RuF_6)_2$ were obtained by crystallizing reaction products from reactions between $M(RuF_6)_2$ (M = Cu, Ni) and XeF_2 at the molar ratio 1:2. The crystals of $[Cu(XeF_2)_2](RuF_6)_2$ formed as colorless needles, while those of $[Ni(XeF_2)_2](RuF_6)_2$ appeared as green needles. The crystal data and refinement results for both compounds are given in **Table 4**.

Crystal structures of $[Cu(XeF_2)_2](RuF_6)_2$ and $[Ni(XeF_2)_2](RuF_6)_2$ are isotypic, which is expected since Ni^{2+} has a similar radius (0.69 Å) to Cu^{2+} (0.71 Å).[33] They crystallize in the monoclinic space group $P2_1/c$. $[Cu(XeF_2)_2](SbF_6)_2$ and $[Ni(XeF_2)_2](IrF_6)_2$ also crystallize in this space group.[6,8] In this group of crystal structures, the metal cation is coordinated to six F atoms. Two F atoms are provided from two XeF_2 ligands, while the remaining four F atoms belong to AF_6 units (A = Ru, Sb, Ir). The XeF_2 molecules are nonbridging, while the AF_6 units are bridging, meaning they connect the metal cations (two cations are connected by two AF_6 units via F atoms in cis positions) into infinite $-[M(\eta^1-XeF_2)_2]-(cis-\eta^2-AF_6)_2-[M(\eta^1-XeF_2)_2]-$ chains along the a-axis (**Figure 4**). The chains are interconnected by Xe···F(A) contacts (noble gas or aerogen bonds[34]), which determine the packing in the crystal structure (**Figure 5**).[8] Aerogen bonds between and within chains, involving electronegative F atoms and more electropositive Xe atoms, cause the F—Xe—F bond angle to deviate from the ideal 180° observed in free XeF_2 molecule (in the case of M = Cu and A = Ru, the F—Xe−F bond angle is 179.0(2)°, and in the case of M = Ni and A = Ru, it is 179.7(1)°).[34–36] Crystal structures of $[Cu(XeF_2)_2](RuF_6)_2$ and

Research Article
doi.org/10.1002/ejic.202500275

Chemistry Europe
European Chemical Societies Publishing

Table 4. Crystal data and structure refinement for $[Cu(XeF_2)_2](RuF_6)_2$ and $[Ni(XeF_2)_2](RuF_6)_2$.

Parameter	Value	Value
Formula	$[Cu(XeF_2)_2](RuF_6)_2$	$[Ni(XeF_2)_2](RuF_6)_2$
Fw [g mol^{-1}]	832.28	827.45
T [K]	150	150
Crystal system	Monoclinic	Monoclinic
Space group	$P2_1/c$	$P2_1/c$
a [Å]	5.4522(4)	5.3883(3)
b [Å]	9.1471(6)	14.7016(9)
c [Å]	14.3707(9)	9.1093(5)
α [°]	90	90
β [°]	92.780(6)	91.786(5)
γ [°]	90	90
V [Å^3]	715.85(8)	721.26(7)
Z	2	2
D_{calcd} [g cm^{-3}]	3.861	3.810
λ [Å]	0.71073	0.71073
μ [mm^{-1}]	8.372	8.140
GOF[a]	1.207	1.083
R_1[b]	0.0311	0.0242
wR_2[c]	0.0734	0.0489

[a]GOF $= \left[\sum w(F_o^2 - F_c^2)^2/(N_o - N_p)\right]^{1/2}$, where N_o = no. of refines and N_p = no. of refined parameters. [b]$R_1 = \sum||F_o| - |F_c||/\sum|F_o|$. [c]$wR_2 = [\sum w(F_o^2 - F_c^2)^2/\sum(w(F_o^2)^2]^{1/2}$.

$[Ni(XeF_2)_2](RuF_6)_2$ are similar to the crystal structure of $[Mg(XeF_2)_2](AsF_6)_2$. The structural motif of all these structures is essentially the same. The shortest metal−metal distances within each chain define the *a* parameter in each structure. The most ordered $[Mg(XeF_2)_2](AsF_6)_2$ compound crystallizes in the orthorhombic *Pbam* space group.[37] Small shift of neighbor chains results in a decrease in symmetry to monoclinic. Depending on the shift direction, two derivative structures are formed (Table 4). These small changes could be attributed to the differences in aerogen bonds Xe···F(A).[34]

The coordination polyhedron of the six-coordinated Cu atom is usually an elongated octahedron.[27] In $[Cu(XeF_2)_2](RuF_6)_2$, however, an example of a compressed octahedron is observed, and $[Ni(XeF_2)_2](RuF_6)_2$ is no exception: the Cu−F(Xe) (Ni−F(Xe)) bonds are shorter than the Cu−F(Ru) (Ni−F(Ru)) bonds. The same can be observed in the isotypic crystal structures of $[Cu(XeF_2)_2](SbF_6)_2$ and $[Ni(XeF_2)_2](IrF_6)_2$ (**Table 5**).[6,8]

From the comparison of the M—F(A) bond lengths (Table 5), it can be observed that in the Ni compounds, the bond lengths are approximately the same whether A = Ru or A = Ir. In contrast, the differences are larger in the Cu compounds—the difference is more pronounced when A = Ru than when A = Sb.[6,8]

In the RuF_6 octahedral units, the Ru—F(M) bonds are longer than the Ru—F bonds (Table 5). Similar to the comparison of M—F(A) bonds in the MF_6 units, the same trend is also observed in the comparison of bonds in the AF_6 units: in Ni compounds, bonds of the same type (A—F(M) or A—F) are similarly long both for A = Ru and A = Ir. In contrast, in Cu compounds, the differences in the bond lengths of bonds of the same type are greater (compared to Ni compounds), both for A = Ru and A = Sb.[6,8]

The M—F(Xe) distances are shorter in Cu compounds than in Ni compounds, which means that XeF_2 coordinates more strongly to Cu than to Ni (Table 5). This effect might also be attributed to the difference in electron affinity, with Cu^{2+} exhibiting a higher value (20.29 eV) compared to Ni^{2+} (18.17 eV).[38] Consequently, the Xe—F(M) bonds are shorter in the Ni compounds than in the Cu compounds, while the Xe—F bonds are longer in the Ni compounds than in the Cu compounds (Table 5). Such a difference in bond length between Xe—F and Xe—F(M) bonds in the Cu compounds is due to the high electron affinity of the Cu^{2+} ion. The largest difference in these bond lengths among all known $[M^{x+}(XeF_2)_n](A)_x$ compounds (where M = Mg−Ba, Zn, Cd, Pb, La, Nd, A = BF_4, PF_6, etc.) is found in $[Cu(XeF_2)_2](SbF_6)_2$.[8,19]

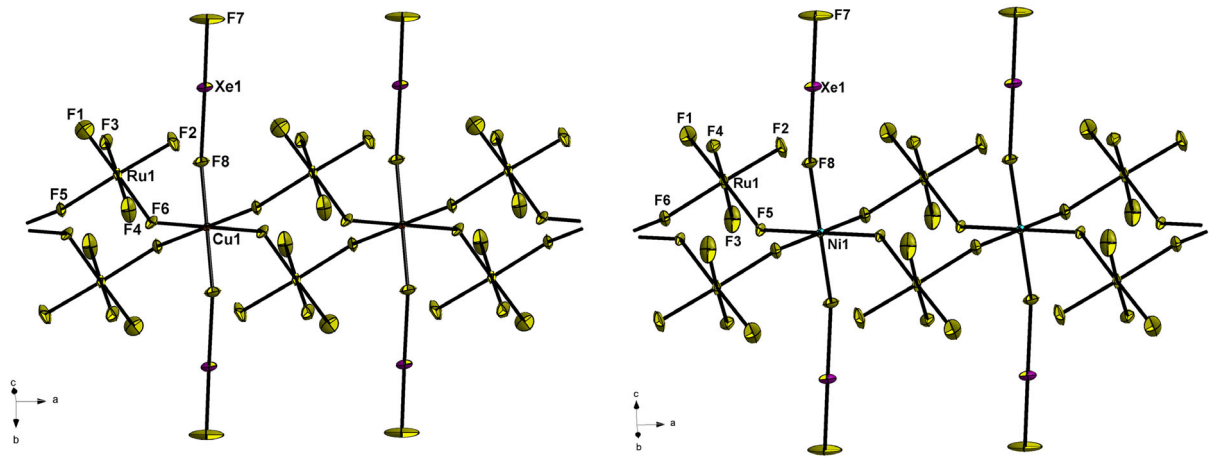

Figure 4. Representation of a part of infinite chains $-[M(\eta^1 - XeF_2)_2]-(cis-\eta^2 - RuF_6)_2-[M(\eta^1 - XeF_2)_2]-$ (M = Cu, Ni) along the *a*-axis. The atoms in the RuF_6 unit are labeled such that the bond Ru1—F1 is the shortest, while the bond Ru—F6 is the longest. Thermal ellipsoids are drawn at a 50% probability level.

Research Article
doi.org/10.1002/ejic.202500275

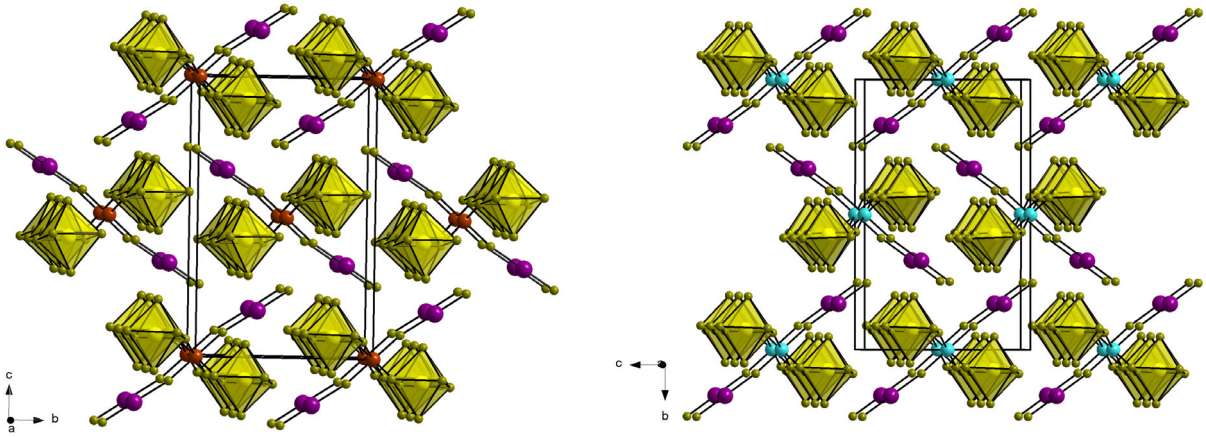

Figure 5. Packing in the crystal structures of $[Cu(XeF_2)_2](RuF_6)_2$ (left) and $[Ni(XeF_2)_2](RuF_6)_2$ (right). The colors of the atoms are Xe–purple, F–dark yellow, Ru–yellow, Cu–brown, and Ni–aqua. In both cases, the unit cell is also shown.

Table 5. A comparison of M—F(Xe) and M—F(A) (MF_6 octahedron), A—F(M) and A—F (AF_6 octahedron) and Xe—F(M) and Xe—F bond lengths (Å) in $[Cu(XeF_2)_2](AF_6)_2$ (A = Ru, Sb) and $[Ni(XeF_2)_2](AF_6)_2$ (A = Ru, Ir).

Bonding atoms	M = Cu		M = Ni	
	A = Ru	A = Sb[a)]	A = Ru	A = Ir[b)]
M—F(Xe)	2 × 1.878(3)	2 × 1.857(5)	2 × 1.948(2)	2 × 1.938(6)
M—F(A)	1.956(3), 1.956(4)	2 × 2.090(5)	2 × 2.010(2)	2 × 2.016(9)
	2 × 2.242(3)	2 × 2.123(5)	2 × 2.020(2)	2 × 2.023(7)
A—F(M)	1.875(3)	1.891(5)	1.905(2)	1.921(7)
	1.913(3)	1.917(5)	1.910(2)	1.934(7)
A—F	1.808(4)	1.841(6)	1.815(2)	1.843(8)
	1.824(4)	1.843(6)	1.822(2)	1.852(8)
	1.836(4)	1.861(6)	1.826(3)	1.858(8)
	1.837(4)	1.870(6)	1.836(2)	1.861(8)
Xe—F(M)	2.091(3)	2.102(5)	2.064(2)	2.078(6)
Xe—F	1.911(4)	1.906(5)	1.925(2)	1.920(7)

[a)]Ref. [8]. [b)]Ref. [6].

2.2.2. Raman Characterization

In Raman spectra of the $[Cu(XeF_2)_2](RuF_6)_2$ and $[Ni(XeF_2)_2](RuF_6)_2$ crystal (**Figure 6**), a doublet is observed in the spectral region characteristic for the Xe—F stretching vibrations of nonbridging XeF_2 molecules. For M = Cu, these bands are located at 579 and 588 cm^{-1}, while for M = Ni, they are observed at 566 and 576 cm^{-1}. A doublet in the same region is also found in the Raman spectrum of $[Cu(XeF_2)_2](SbF_6)_2$, where the Xe—F vibrations are located at 582 and 591 cm^{-1}. The doublet, or splitting, results from weak vibrational coupling of the XeF_2 molecules within the unit cell.[8] The Xe—F bond vibrations for the Cu compound appear at higher wavenumbers than for the Ni compound. This is due to the Cu—F(Xe) bonds being shorter (stronger bonds) than Ni—F(Xe) bonds, which also results in shorter Xe—F bonds (Table 5). The stronger and consequently shorter the bond, the higher the corresponding vibrational wavenumber. Due to the distortion of the RuF_6 octahedron in coordination compounds, similar to what is observed in the salts $M(RuF_6)_2$, a greater number of bands is present for vibrations in the RuF_6 unit than would be expected for an ideal O_h symmetry. The bands corresponding to Ru—F and Ru—F(M) bond vibrations appear below 300 and above 600 cm^{-1}. These vibrations are derived from ν_1 (stretching), ν_2 (stretching), and ν_5 (bending) vibrational modes of the octahedral $[RuF_6]^-$. **Table 6** provides the vibrational assignments for $[Cu(XeF_2)_2](RuF_6)_2$ and $[Ni(XeF_2)_2](RuF_6)_2$, along with a comparison to the vibrational assignments of $M(RuF_6)_2$ (M = Cu, Ni). The assignments of the bands of vibrations in RuF_6 octahedron in coordination compounds are based on the position of bands in the Raman spectra of $M(RuF_6)_2$ salts (M = Cu, Ni), as well as on the vibrational modes of related octahedral $[AF_6]^-$ anions (A = Sb, Ta, Nb, etc.).[30] The Raman spectra of the powdered products of the reaction between $M(RuF_6)_2$ (M = Cu, Ni) and $2XeF_2$ are provided in the Supporting Information (Figure S2 and S3, Supporting Information). In both cases, the starting compound $M(AF_6)_2$ is present alongside the desired product.

2.3. Crystal Structure and Raman Characterization of $[M(XeF_2)_6](RuF_6)_2$ (M = Cu, Ni)

Just one crystal of $[Cu(XeF_2)_6](RuF_6)_2$ was obtained by crystallizing reaction products from reaction between $Cu(RuF_6)_2$ and XeF_2 in the molar ratio 1:9. Crystals of $[Ni(XeF_2)_6](RuF_6)_2$ were obtained by crystallizing reaction products from reaction between $Ni(RuF_6)_2$ and XeF_2 in the molar ratio 1:12. The crystal of $[Cu(XeF_2)_6](RuF_6)_2$ formed as colorless needle, while those of $[Ni(XeF_2)_2](RuF_6)_2$ appeared as colorless plates. The crystal data and refinement results for both compounds are given in **Table 7**.

$[Cu(XeF_2)_6](RuF_6)_2$ and $[Ni(XeF_2)_6](RuF_6)_2$ crystallize in different space groups, $[Cu(XeF_2)_6](RuF_6)_2$ crystallizes in the triclinic space group $P\bar{1}$, while $[Ni(XeF_2)_6](RuF_6)_2$ crystallizes in the trigonal space group $R\bar{3}$. This is not consistent with expectations based on the similar ionic radii of Cu^{2+} and Ni^{2+} and the fact that the crystal structures of $[Cu(XeF_2)_2](RuF_6)_2$ and $[Ni(XeF_2)_2](RuF_6)_2$ are isotypic.

Research Article
doi.org/10.1002/ejic.202500275

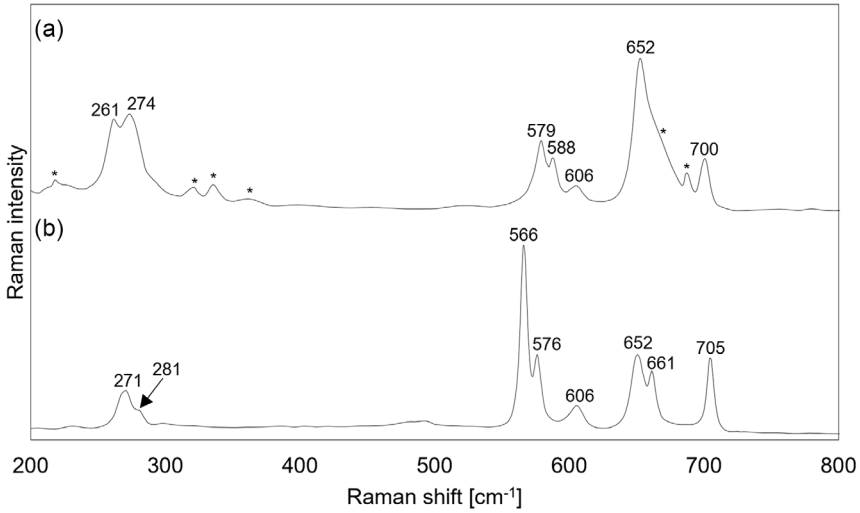

Figure 6. Raman spectra of a) $[Cu(XeF_2)_2](RuF_6)_2$ and b) $[Ni(XeF_2)_2](RuF_6)_2$ recorded on a single crystal. Raman spectrum of $[Cu(XeF_2)_2](RuF_6)_2$ was recorded on a single crystal in perfluorodecalin (bands marked with an asterisk belong to perfluorodecalin), while Raman spectrum of $[Ni(XeF_2)_2](RuF_6)_2$ was recorded through a quartz capillary..

Table 6. Comparison of the Raman spectra assignments of $[M(XeF_2)_2](RuF_6)_2$ and $M(RuF_6)_2$ (M = Cu, Ni).

$[Cu(XeF_2)_2](RuF_6)_2$	$Cu(RuF_6)_2$	Assignment	$[Ni(XeF_2)_2](RuF_6)_2$	$Ni(RuF_6)_2$	Assignment
700 (28)	742 (100)	ν_1[a])(RuF_6)	705 (58)	742 (100)	ν_1[a])(RuF_6)
652 (100)	698 (45)	ν_1[a])(RuF_6)	661 (30)	698 (65)	ν_1[a])(RuF_6)
606 (10)	686 (67)	ν_1[a])(RuF_6)	652 (70)	691 (59)	ν_1[a])(RuF_6)
	650 (43)	ν_1[a])(RuF_6)	606 (16)	647 (29)	ν_1[a])(RuF_6)
588 (21)		ν(Xe–F)	576 (61)		ν(Xe–F)
579 (45)		ν(Xe–F)	566 (100)		ν(Xe–F)
274 (23)	281 (55)	ν_5[b])(RuF_6)	281 (11)	310 (6)	ν_5[b])(RuF_6)
261 (21)	232 (8)	ν_5[b])(RuF_6)	271 (39)	292 (14)	ν_5[b])(RuF_6)
				281 (61)	ν_5[b])(RuF_6)
				242 (16)	ν_5[b])(RuF_6)
				226 (8)	ν_5[b])(RuF_6)

[a])Vibrations derived from ν_1 mode of the octahedral $[RuF_6]^-$. [b])Vibrations derived from ν_5 mode of the octahedral $[RuF_6]^-$.

2.3.1. Crystal Structure of $[Ni(XeF_2)_6](RuF_6)_2$

Crystal structure of $[Ni(XeF_2)_6](RuF_6)_2$ is isotypic to the crystal structures of $[M(XeF_2)_6](SbF_6)_2$ (M = Cu, Zn). The metal cation is homoleptically coordinated by six fluorine atoms from the non-bridging XeF_2 ligands. Since high-spin Ni(II) is not Jahn–Teller active, the metal center adopts a regular octahedral (O_h) geometry (**Figure 7**), as expected, with all Ni–F(Xe) bonds being 1.974(3) Å long.[28] For comparison, the bond lengths in the CuF_6 and ZnF_6 octahedral units of the isotypic crystal structures are 1.979(3) and 1.994(5) Å, respectively. The Ni−F(Xe) bond lengths are therefore similar to Cu−F(Xe) and shorter than the Zn−F(Xe) bond lengths. In Ni compound, Xe−F bonds are 1.935(3) Å long, while Xe−F(Ni) bonds are 2.088(3) Å long. For comparison, the Xe−F bonds in the isotypic crystal structures are 1.934(4) Å (M = Cu) and 1.931(5) (M = Zn) Å long, while the Xe−F(M) bonds are 2.083(3) Å (M = Cu) and 2.078(5) Å (M = Zn) long. The Xe—F and Xe—F(M) bond lengths in the isotypic crystal structures are therefore similar.

Discrete anions $[RuF_6]^-$ also have an octahedral geometry (Figure 7). Although they are not coordinated to the metal center, the distance between Ru and F atoms is not equal; instead, they are of two different lengths, which is likely due to electrostatic interactions in the crystal structure. Three Ru—F bonds are 1.842(3) Å long, and the other three are 1.852(3) Å long. The same applies to the octahedra $[SbF_6]^-$ in isotypic crystal structures, where three bonds are shorter and three are longer (M = Cu: 1.832(4) and 1.862(4) Å, M = Zn: 1.833(6) and 1.862(5) Å).[7]

The $[Ni(XeF_2)_6]^{2+}$ cations are connected with the $[RuF_6]^-$ anions by aerogen bonds Xe···F(Ru).[34] These bonds determine the packing in the crystal structure (**Figure 8**) and are the reason why the F—Xe—F angle deviates from 180°, as seen in the free

Research Article
doi.org/10.1002/ejic.202500275

Table 7. Crystal data and structure refinement for $[Cu(XeF_2)_6](RuF_6)_2$ and $[Ni(XeF_2)_6](RuF_6)_2$.

Parameter	Value	Value
Formula	$[Cu(XeF_2)_6](RuF_6)_2$	$[Ni(XeF_2)_6](RuF_6)_2$
Fw [g mol^{-1}]	1509.48	1504.65
T [K]	150	150
Crystal system	Triclinic	Trigonal
Space group	$P\bar{1}$	$R\bar{3}$
a [Å]	9.142(2)	9.938(2)
b [Å]	10.385(2)	9.938(2)
c [Å]	13.256(1)	22.040(4)
α [°]	89.71(1)	90
β [°]	89.59(1)	90
γ [°]	87.83(1)	120
V [Å^3]	1257.6(3)	1885.3(8)
Z	2	3
D_{calcd} [g cm^{-3}]	3.986	3.976
λ [Å^{-1}]	0.71073	0.71073
μ [mm^{-1}]	10.136	10.045
GOF[a]	1.066	1.095
R_1[b]	0.0298	0.0256
wR_2[c]	0.0799	0.0582

[a] $GOF = [\Sigma w(F_o^2 - F_c^2)^2/(N_o - N_p)]^{1/2}$, where N_o = no. of refines and N_p = no. of refined parameters. [b] $R_1 = \sum ||F_o| - |F_c|| / \sum |F_o|$. [c] $wR_2 = [\sum w(F_o^2 - F_c^2)^2 / \sum (w(F_o^2)^2]^{1/2}$.

XeF_2 molecule. The F—Xe—F angle in $[Ni(XeF_2)_6](RuF_6)_2$ is 177.9(1)°. For comparison, in isotypic crystal structures, the F—Xe—F angle is 179.3(2)° for M = Cu and 178.9(2)° for M = Zn.[7,35]

2.3.2. Crystal Structure of $[Cu(XeF_2)_6](RuF_6)_2$

The crystal structure of $[Cu(XeF_2)_6](RuF_6)_2$ differs from the above-mentioned crystal structures, although it also contains a homoleptic cation $[M(XeF_2)_6]^{2+}$.

There are two different CuF_6 octahedral units in the crystal structure (**Figure 9**), and in both, the JT effect is observed. There are three pairs of bonds with different lengths in each unit, with one pair standing out in length (marked in bold in **Table 8**) and indicating an elongated shape of the octahedron. This differs from the analogous compound $[Cu(XeF_2)_6](SbF_6)_2$, where no JT effect is observed, as all Cu—F bond lengths are identical.[7] The JT effect is sometimes not observed during the determination of crystal structures, but this does not necessarily mean that it is absent. One possible reason is structural disorder, where a defined long axis is randomly distributed along the three directions relative to the unit cell axes (static disorder).

Another possibility is the presence of sufficient thermal motion, which allows the long and short bonds to exchange over time. In this case, the disorder is dynamic, as the Cu—ligand bond lengths become temperature-dependent.[27,39]

The presence of the JT effect in $[Cu(XeF_2)_6](RuF_6)_2$ and its apparent absence in $[Cu(XeF_2)_6](SbF_6)_2$ and therefore the difference in the crystal structure could be attributed to the fact that the crystal structures were determined at different temperatures. Specifically, the crystal structure of $[Cu(XeF_2)_6](RuF_6)_2$ was obtained at 150 K, whereas that of $[Cu(XeF_2)_6](SbF_6)_2$ was obtained at 200 K. At 200 K, thermal motion in $[Cu(XeF_2)_6](SbF_6)_2$ may be sufficient to mask or average out the JT distortion.[7]

The crystal structure also contains two different RuF_6 octahedral units. In each of them, all Ru—F bond lengths are different (Table 8). It is possible that the distortion of otherwise discrete octahedra occurs due to the aerogen bonds Xe···F(A).[34]

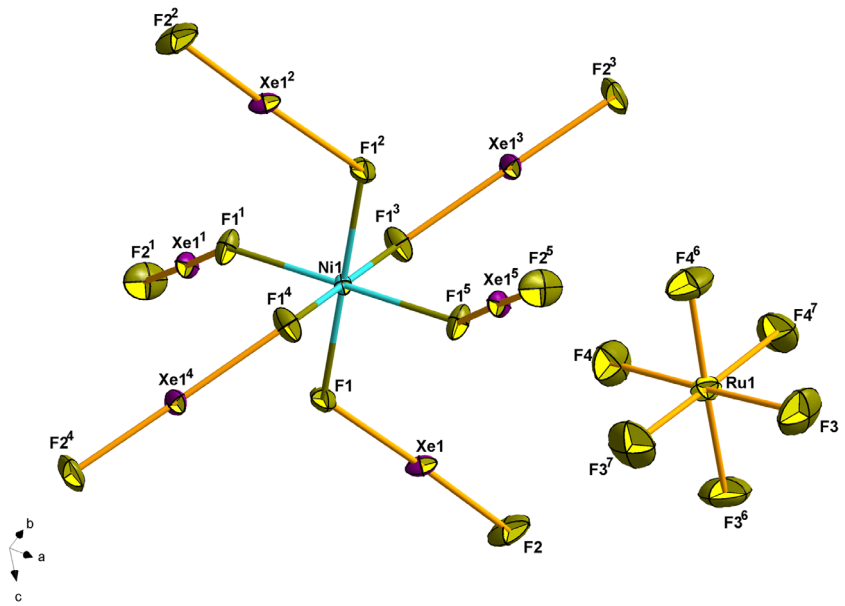

Figure 7. The relative positions of $[Ni(XeF_2)_6]^{2+}$ octahedron with respect to the $[RuF_6]^-$ octahedron. Symmetry operations used for generation of equivalent atoms: [1] +*y*, −*x* + *y*, 1 − *z*; [2] −*x*, −*y*, 1 − *z*; [3] −*y* + *x*, +*x*, 1 − *z*; [4] +*y* − *x*, −*x*, +*z*; [5] −*y*, +*x* − *y*, +*z*; [6] 1 + *y* − *x*, 1 − *x*, +*z*; [7] 1 − *y*, +*x* − *y*, +*z*.

Research Article
doi.org/10.1002/ejic.202500275

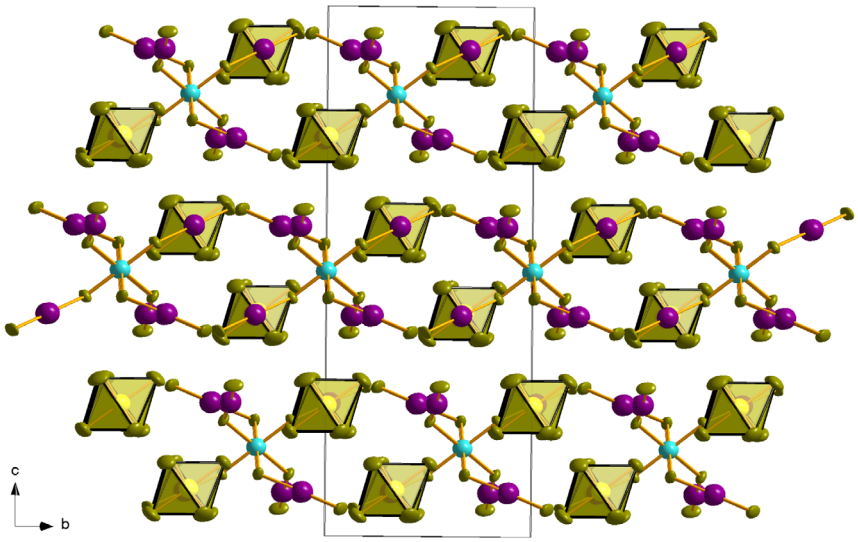

Figure 8. Packing in the crystal structure of $[Ni(XeF_2)_6](RuF_6)_2$. The atom colors are Xe–violet, F–dark yellow, Ru–yellow, and Ni–aqua. The unit cell is also shown.

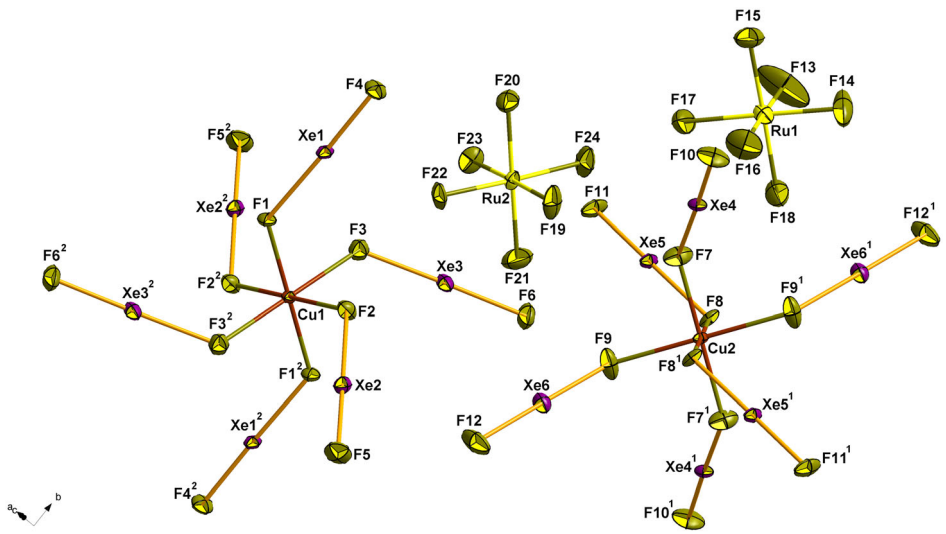

Figure 9. The relative positions of $[Cu(XeF_2)_6]^{2+}$ octahedra with respect to the $[RuF_6]^-$ octahedra. Symmetry operations used for generation of equivalent atoms: $^1-x, 1-y, -z$; $^2 1-x, -y, 1-z$.

Table 8. A comparison of the bond lengths (Å) in the CuF_6 and RuF_6 octahedral units of $[Cu(XeF_2)_6](RuF_6)_2$.

CuF_6 octahedron				RuF_6 octahedron			
M = Cu1		M = Cu2		A = Ru1		A = Ru2	
Bonding atoms	Length	Bonding atoms	Length	Bonding atoms	Length	Bonding atoms	Length
Cu1–F1	1.907(4)	Cu2–F7	1.917(5)	Ru1–F13	1.825(6)	Ru2–F19	1.838(5)
Cu1–F2	1.957(4)	Cu2–F8	1.949(4)	Ru1–F14	1.839(6)	Ru2–F20	1.845(5)
Cu1–F3	**2.167(5)**	Cu2–F9	**2.154(5)**	Ru1–F15	1.843(5)	Ru2–F21	1.849(6)
				Ru1–F16	1.846(6)	Ru2–F22	1.854(4)
				Ru1–F17	1.847(6)	Ru2–F23	1.861(5)
				Ru1–F18	1.857(6)	Ru2–F24	1.862(5)

Research Article
doi.org/10.1002/ejic.202500275

The Xe—F and Xe—F(Cu) bond lengths are comparable to the Xe—F and Xe—F(M) bond lengths in other crystal structures containing homoleptic cations. In each CuF_6 octahedral unit, there are three pairs of different Xe—F and Xe—F(Cu) bonds. The lengths of the Xe—F(Cu) bonds range from 2.033 to 2.126 Å, while the lengths of Xe—F range from 1.916 to 1.959 Å.

Aerogen bonds Xe···F(Ru) between $[Cu(XeF_2)_6]^{2+}$ cations and $[RuF_6]^-$ anions determine the packing in the crystal structure (**Figure 10**).[34] Similar to the Ni compound, deviations in the F—Xe—F bond angle from 180° are also observed in this case. The values of the F—Xe—F angles range from 178.1(2)° to 179.0(2)°.

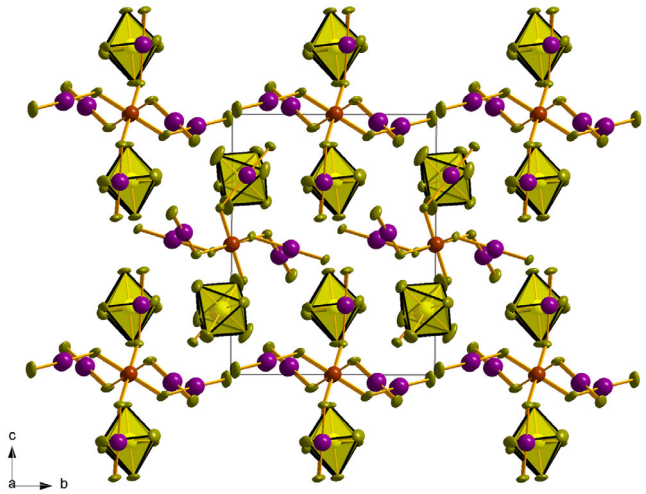

Figure 10. Packing in the crystal structure of $[Cu(XeF_2)_6](RuF_6)_2$. The atom colors are Xe–violet, F–dark yellow, Ru–yellow, and Cu–brown. The unit cell is also shown.

2.3.3. Raman Characterization of $[Ni(XeF_2)_6](RuF_6)_2$

In the Raman spectrum of the powdered product (**Figure 11**, **Table 9**) of the reaction between $Ni(RuF_6)_2$ and an excess of XeF_2 (1:12), several phases are observed: excess of XeF_2 at 497 cm^{-1}, a residue of starting compound $Ni(RuF_6)_2$ (weak bands at 281, 691, 698 and 742 cm^{-1}; the band at 647 cm^{-1} is too strong to be attributed only to $Ni(RuF_6)_2$) and Ni coordination compounds with varying numbers of differently coordinated XeF_2 (bridging and nonbridging) molecules.

The band at 562 cm^{-1} can be assigned to Xe—F stretching vibrations of nonbridging XeF_2, while the band at 422 cm^{-1} can be attributed to the stretching vibration of the Xe—F(Ni) bond. In the Raman spectra of compounds with isotypic crystal structure, a band corresponding to Xe–F bond vibrations also appears at a wavenumber around 560 cm^{-1} (for $[Cu(XeF_2)_6](SbF_6)_2$ at 560 and for $[Zn(XeF_2)_6](SbF_6)_2$ at 563 cm^{-1}).[7]

Bands above 600 and below 300 cm^{-1} can be assigned to vibrations in RuF_6 units. These vibrations are derived from ν_1, ν_2, and ν_5 vibrational modes of the octahedral $[RuF_6]^-$.

Table 9. Tentative Raman assignments for different compounds in the powdered product after the reaction between $Ni(RuF_6)_2$ and an excess of XeF_2.

Excess of XeF_2	$Ni(RuF_6)_2$	$[Ni(XeF_2)_6](RuF_6)_2$
497 (ν(Xe–F))	742 (ν_1[a])(RuF_6))	660 (ν_1[a])(RuF_6))
	698 (ν_1[a])(RuF_6))	647 (ν_1[a])(RuF_6))
	691 (ν_1[a])(RuF_6))	562 (ν(Xe–F))
	281 (ν_5[b])(RuF_6))	422 (ν(Xe–F(M))
		262 (ν_5[b])(RuF_6))

[a]Vibrations derived from ν_1 mode of the octahedral $[RuF_6]^-$. [b]Vibrations derived from ν_5 mode of the octahedral $[RuF_6]$.

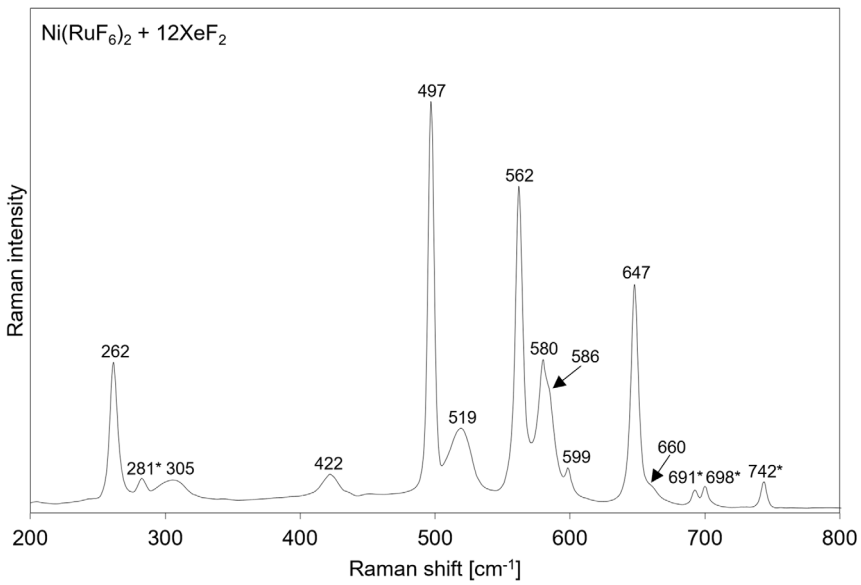

Figure 11. Raman spectrum of the powdered product of the reaction between $Ni(RuF_6)_2$ and an excess of XeF_2. Raman spectrum was recorded through a quartz capillary. The bands marked with an asterisk (*) belong to the starting compound $Ni(RuF_6)_2$.

Research Article
doi.org/10.1002/ejic.202500275

Chemistry Europe
European Chemical Societies Publishing

Remaining bands (519, 580, 586, and 599 cm^{-1}) most probably belong to different XeF_2 coordination compounds (or even by-products, e.g., $[Xe_2F_3][RuF_6]\cdot XeF_2$), that we were not able to crystallize. Despite the absence of some bands (271, 566, 576, 606, 652, 661, and 705 cm^{-1}) compared to the Raman spectrum of the crystal (Figure 6b), $[Ni(XeF_2)_2](RuF_6)_2$ also crystallized from this mixture. The reason may be partial decomposition of $[Ni(XeF_2)_6](RuF_6)_2$ during prolonged crystallization.

2.3.4. Raman Characterization of $[Cu(XeF_2)_6](RuF_6)_2$

In the Raman spectrum of the powdered product (**Figure 12**a, **Table 10**) of the reaction between $Cu(RuF_6)_2$ and an excess of XeF_2 (1:8), the following phases were observed: $[Xe_2F_3][RuF_6]\cdot XeF_2$ and products with 1:2, 1:4, and 1:6 stoichiometry. Bands at wavenumbers 264, 506, 517, 579, 588, and 650 cm^{-1} (with only a minor band missing at 667 cm^{-1}, which may be overlapped by the broad one at 650 cm^{-1}) suggest, based on literature data, the formation of $[Xe_2F_3][RuF_6]\cdot XeF_2$. The bands at 506 and 517 cm^{-1} can be attributed to the XeF_2 weakly associated with the $[Xe_2F_3]^+$ cations and $[RuF_6]^-$ anions, while the bands at 579 and 588 cm^{-1} can be assigned to Xe—F stretching vibrations in the $[Xe_2F_3]^+$ cation. The bands at 264 and 650 cm^{-1} can be attributed to vibrations in the $[RuF_6]^-$ anions.[40]

The Raman spectrum of the compound $[Cu(XeF_2)_2](RuF_6)_2$ is similar to that of $[Xe_2F_3][RuF_6]$. Since $[Cu(XeF_2)_2](RuF_6)_2$ (beside $[Cu(XeF_2)_6](RuF_6)_2$) also crystallized during the crystallization of the product mixture, it can be assumed that this compound was also present in the powder product. This assumption is supported by the additional bands at 606 and 700 cm^{-1}, which were also observed in the Raman spectrum of $[Cu(XeF_2)_2](RuF_6)_2$ crystal (Figure 6a).

The bands at 561 and 569 cm^{-1} are within the range of wavenumbers characteristic of Xe—F stretching vibrations of nonbridging XeF_2 molecules. According to literature data, this suggests the possible presence of both $[Cu(XeF_2)_4](RuF_6)_2$ ($[Cu(XeF_2)_4](SbF_6)_2$ shows a doublet at 562 and 578 cm^{-1}) and $[Cu(XeF_2)_6](RuF_6)_2$ ($[Cu(XeF_2)_6](SbF_6)_2$ shows a band at 560 cm^{-1}).[7,8]

For comparison, the Raman spectrum of the powdered product of the reaction between $Cu(RuF_6)_2$ and $4XeF_2$ is added (Figure 12b). The bands corresponding to Xe—F bond vibrations appear at the same wavenumbers in both spectra. The same

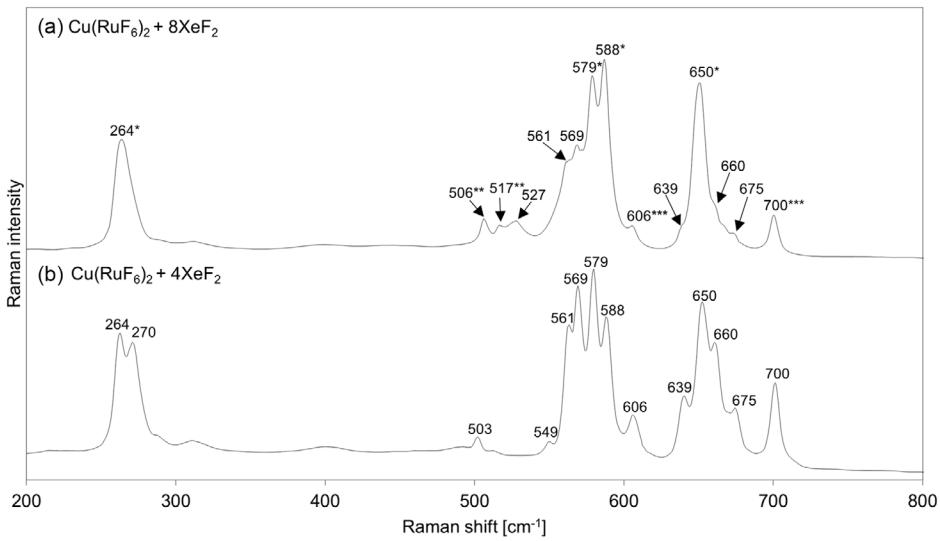

Figure 12. a) Raman spectrum of the powdered product of the reaction between $Cu(RuF_6)_2$ and an excess of XeF_2 and b) Raman spectrum of the powdered product of the reaction between $Cu(RuF_6)_2$ and $4XeF_2$. Bands marked with (**) are characteristic only of $[Xe_2F_3][RuF_6]\cdot XeF_2$, those marked with (*) are characteristic of both $[Xe_2F_3][RuF_6]\cdot XeF_2$ and $[Cu(XeF_2)_2](RuF_6)_2$, while bands marked with (***) are characteristic only of $[Cu(XeF_2)_2](RuF_6)_2$. Both Raman spectra were recorded through a quartz capillary.

Table 10. Tentative Raman assignments for different compounds (species*) in the powdered product after the reaction between $Cu(RuF_6)_2$ and excess of XeF_2.

$[Xe_2F_3][RuF_6]\cdot XeF_2$[c)]	$[Cu(XeF_2)_2](RuF_6)_2$	$[Cu(XeF_2)_4](RuF_6)_2$	$[Cu(XeF_2)_6](RuF_6)_2$	$\nu(RuF_6)$*
650 (ν_1[a)](RuF_6))	700 (ν_1[a)](RuF_6))	569 (ν(Xe-F))	561 (ν(Xe-F))	675 (ν_1[a)])
588 (ν(Xe-F))	650 (ν_1[a)](RuF_6))			660 (ν_1[a)])
579 (ν(Xe-F))	606 (ν_1[a)](RuF_6))			639 (ν_1[a)])
517 (ν(F-Xe-F))	588 (ν(Xe-F))			
506 (ν(F-Xe-F))	579 (ν(Xe-F))			
264 (ν_5[b)](RuF_6))	264 (ν_5[b)](RuF_6))			

[a)]Vibrations derived from ν_1 mode of the octahedral $[RuF_6]^-$. [b)]Vibrations derived from ν_5 mode of the octahedral $[RuF_6]^-$. [c)]Ref. [40].

Research Article
doi.org/10.1002/ejic.202500275

applies to the vibrations of bonds in RuF_6 units. From this, it can be concluded that both compounds $[Cu(XeF_2)_4](RuF_6)_2$ and $[Cu(XeF_2)_6](RuF_6)_2$ could be present in the powdered products. Given that all attempts to prepare crystals of $[Cu(XeF_2)_4](RuF_6)_2$ were unsuccessful, and that the Raman spectrum of the $[Cu(XeF_2)_6](RuF_6)_2$ crystal was not obtained, it is not possible to definitively assign which bands correspond to $[Cu(XeF_2)_4](RuF_6)_2$ and which to $[Cu(XeF_2)_6](RuF_6)_2$. Additionally, the presence of two distinct CuF_6 octahedra in $[Cu(XeF_2)_6](RuF_6)_2$ further complicates the assignments of the Raman bands.

The compound $[Cu(XeF_2)_6](RuF_6)_2$ is not stable under dynamic vacuum. Figure S4, Supporting Information, shows the difference between the Raman spectrum of the powdered product of the reaction between $Cu(RuF_6)_2$ with an excess of XeF_2 before ((a)) and after ((b)) 450 min of pumping under dynamic vacuum. The Raman spectrum after pumping under dynamic vacuum matches the Raman spectrum of the compound $[Cu(XeF_2)_2](RuF_6)_2$, while the bands indicating the presence of $[Cu(XeF_2)_6](RuF_6)_2$ are no longer observed. The remaining powder was crystallized, and the crystallized product was $[Cu(XeF_2)_2](RuF_6)_2$, indicating that this compound is stable under dynamic vacuum conditions.

The literature suggests that at least two reactions are in equilibrium in the system $Cu(SbF_6)_2$–XeF_2, or $Cu(RuF_6)_2$–XeF_2 analogously for this paper. First reaction leads to the formation of $[Cu(XeF_2)_6](RuF_6)_2$, while the second results in the formation of $[Xe_2F_3][RuF_6]$ and CuF_2 (Equation (2)).[7]

$$Cu(RuF_6)_2 + nXeF_2 \xrightarrow[298K]{aHF} x[Cu(XeF_2)_6](RuF_6)_2 + y[Xe_2F_3][RuF_6] + zCuF_2 \quad (2)$$

In the case where A = Sb, the equilibrium was confirmed by the reaction between CuF_2 and $[Xe_2F_3][SbF_6]$, for which the isolated solid was proved to be a mixture of $[Cu(XeF_2)_6](SbF_6)_2$, $[Xe_2F_3][SbF_6]$ and CuF_2.[7]

3. Conclusion

$Cu(RuF_6)_2$ and $Ni(RuF_6)_2$ are the first synthesized compounds of the $M^{II}(Ru^{V}F_6)_2$ type. The syntheses were carried out under UV light. Raman spectra of both powdered products were recorded, while the crystal structure was determined only for $Cu(RuF_6)_2$. Based on known crystal structures of compounds of the general formula $M^{II}(A^{V}F_6)_2$, the crystal structure of $Cu(RuF_6)_2$ belongs to the Type I: layers of CuF_6 and RuF_6 units with common F atoms, where Cu^{2+} cations are connected by RuF_6 units, forming slabs held together by van der Waals forces.[20] Due to the similarity between the Raman spectra of $Cu(RuF_6)_2$ and $Ni(RuF_6)_2$, the latter is also expected to belong to the same crystal structure type. $Cu(RuF_6)_2$ and $Ni(RuF_6)_2$ were used as starting materials for the synthesis of coordination compounds $[M(XeF_2)_n](RuF_6)_2$. Raman spectroscopy was a useful tool to monitor products of the reactions. Compounds with stoichiometries of 1:2 and 1:6 were structurally characterized for both Cu and Ni. The Ni compounds are particularly interesting since the only one example was found recently.[6] The compounds $[Cu(XeF_2)_2](RuF_6)_2$ and $[Ni(XeF_2)_2](RuF_6)_2$ are isostructural with the crystal structures of already known compounds $[Cu(XeF_2)_2](SbF_6)_2$ and $[Ni(XeF_2)_2](IrF_6)_2$.[6,8] In these structures, Cu or Ni atoms are connected via RuF_6 units, forming chains, with two nonbridging XeF_2 molecules coordinated to each metal center. The crystal structures of $[Cu(XeF_2)_6](RuF_6)_2$ and $[Ni(XeF_2)_6](RuF_6)_2$ (1:6 stoichiometry) are not isostructural, despite in both cases the metal center is homoleptically coordinated by XeF_2 molecules. The crystal structure of the Ni compound is isotypic to $[Cu(XeF_2)_6](SbF_6)_2$ and $[Zn(XeF_2)_6](SbF_6)_2$.[7]

4. Experimental Section

When working with aHF, XeF_2, and fluorides, extreme caution must be taken. Reactions should be carried out in a well-ventilated fume hood, and appropriate protective clothing must be worn at all times. Calcium gluconate gel should always be readily available for the immediate treatment of skin exposed to these reagents.[41] Before working with these substances, it was advisable to familiarize oneself with the consequences of accidents and the procedures to follow in case of contact. For more information on the hazards and actions to take in case of contact with aHF, refer to another study.[42]

General Experimental Procedure

System Description

The experimental work was carried out on a vacuum system made from Teflon and nickel components, equipped with pressure gauges (the main pressure gauge was a Monel Helicoid connected to the Teflon part of the vacuum system and has a measuring range from 0 to 1500 torr), traps for capturing HF (made of FEP), moisture (glass traps immersed in liquid nitrogen), and F_2 (soda lime), and vacuum pumps. The vacuum of up to 10^{-3} mbar was achieved using a rotary pump. For higher-vacuum requirements, a diffusion pump was used, which, in combination with the rotary pump, achieved a vacuum of up to 10^{-5} mbar.

General Procedure for Reactions

The reaction vessels were made of FEP (internal diameter of 16 mm), and they were equipped with a Teflon valve and Teflon-covered magnet for mixing. Before use, the reaction vessel must be tested to ensure it was sealed and fluorinated on the vacuum system. For more details on the construction of the reaction vessel (vessel and valve together), refer to the literature.[15] Reactants sensitive to moisture were weighed in a glove box with a water vapor content less than 0.5 ppm in an argon atmosphere. ≈3 mL of solvent (aHF) was added on the vacuum system. After the reaction was complete, the product was isolated by pumping out aHF either at room temperature or, if the compound contained XeF_2, at a temperature below 0 °C to prevent subliming (the reaction vessel was immersed in alcohol cooled with liquid nitrogen to the desired temperature). When the aHF was pumped out, a powder (solid) product remained, which was stored in a glove box until future use.

Crystal Preparation (Crystallization)

Crystallization was carried out in a T-shaped crystallization vessel. It consisted of two parts (arms) connected by the so-called T-piece. The wider arm was of the same dimensions as the reaction vessels,

while the narrower arm was shaped like an inverted "L" with an internal diameter of 4 mm. The material was added to the wide arm. Saturated solution in aHF was decanted into the narrow arm so that the undissolved substance remained in the wide arm. Crystal growth was carried out under a temperature gradient between the narrow arm (higher temperature) and the wide arm (lower temperature). The details of the crystallization process (time, temperature, mass) are provided in Table S1, Supporting Information.

Raman Spectroscopy

Raman spectra with a resolution of 0.5 cm^{-1} were recorded at room temperature on a HORIBA JOBIN YVON LabRam-HR spectrometer equipped with the Olympus BXFM-ILHS microscope. Samples were excited by the 632.8 nm emission line of a He—Ne laser.[9] Raman spectra were recorded for all powdery products and for some products also on single crystals. Raman spectra were recorded either through perfluorodecalin, FEP, or Raman capillary. In the latter case, the substance was added to the capillary in a glove box and sealed with halocarbon grease. To prevent moisture from entering, the capillary was additionally sealed above a flame.

Determination of Crystal Structure

Crystals were immersed in perfluorodecalin (Fluorochem, Cat. Code: 003283, melting point 263 K)) inside a glove box, selected under a microscope, and mounted on the goniometer head of the diffractometer in a cold nitrogen stream. Single-crystal data for $Cu(RuF_6)_2$, $[Cu(XeF_2)_2](RuF_6)_2$, $[Ni(XeF_2)_2](RuF_6)_2$, $[Cu(XeF_2)_6](RuF_6)_2$ and $[Ni(XeF_2)_6](RuF_6)_2$ were collected on a Gemini A diffractometer equipped with an Atlas CCD detector, using graphite monochromated Mo−Kα radiation. The data were treated using the CrysAlisPro software suite program package.[43] Analytical absorption correction was applied. The structure was solved using the SHELXS program.[44] Structure refinement was performed with the SHELXL-2014[45] software, implemented in the program package WinGX.[46] The figures were prepared using the DIAMOND 4.6.8 software.[47] CIF's files can be obtained from Fachinformationszentrum Karlsruhe, 76 344 Eggenstein-Leopoldshafen, Germany (e-mail: crysdata@fiz karlsruhe.de; http://www.fiz-karlsruhe.de/request_for_deposited_data.html) on quoting the appropriate CSD number.[48]

Reagents

Ru powder (ALDRICH, 99.9%), CuF_2 (Thermo Scientific, anhydrous 99.5%), NiF_2 (Thermo Scientific, anhydrous 97%), and elemental F_2 (Solvay Fluor and Derivate GmbH, 99.98%) were used as supplied. Anhydrous HF (Linde AG, 99.995%) was treated with K_2NiF_6 (Advanced Research Chemicals, Inc., 99.9%) several days before use.

Synthesis

The general procedure for carrying out the reaction and crystallization was described in the section "General Experimental Procedure".

Synthesis of $M(RuF_6)_2$ (M = Cu, Ni)

$Cu(RuF_6)_2$ was synthesized from CuF_2 (116 mg, 1.14 mmol), Ru (210 mg, 2.08 mmol), and an excess of F_2. The reactant ratio was $n(CuF_2):n(Ru) = 1.1:2$. Ruthenium powder should not touch the walls of the vessel, but instead, it should be added to the bottom using a long-necked funnel. This prevented the added F_2 from reacting with dry Ru powder, which could lead to a violent reaction and heating of a small part of the vessel, potentially softening it and causing it to fail under high pressures. During the reaction in anhydrous HF (aHF), the heat released was transferred to the solvent.[15] The reactants CuF_2 (white powder) and Ru (gray powder) were very poorly soluble in HF (the solubility of CuF_2 is 0.010 ± 0.005 g per 100 g HF at 12.4 °C[49]). F_2 was added to the cooled reaction vessel (liquid nitrogen) on the vacuum system. The reaction was carried out under UV light, using a medium-pressure mercury lamp (Hg arc lamp, 450 W, Ace Glass). The lamp surface heated up significantly during operation, so it was continuously cooled in a glass immersion well through which cold water flowed.[15] The pressure of F_2 in the reaction vessel was checked every few days. F_2 was added until a noticeable drop in pressure was observed during the checks. The reaction lasted for 13 days at room temperature. After the reaction, the product was isolated. The mass of the dry residue was 602 mg. When weighing $Cu(RuF_6)_2$ for the syntheses of coordination compounds, it was taken into account that the raw product also contained unreacted CuF_2. The mass was calculated based on the mass of the starting Ru. The product was reddish-pink, and it was poorly soluble in aHF.

$Ni(RuF_6)_2$ was synthesized from NiF_2 (108 mg, 1.12 mmol), Ru (205 mg, 2.03 mmol), and an excess of F_2. The reactant ratio was $n(NiF_2):n(Ru) = 1.1:2$. The synthesis and isolation procedure were the same as for the $Cu(RuF_6)_2$ synthesis. The solubility of NiF_2 (yellow powder) in aHF was also poor (0.037 ± 0.002 g per 100 g HF at 11.9 °C[49]). The reaction lasted for 13 days. The isolation procedure was the same as for $Cu(RuF_6)_2$. The mass of the dry residue was 518 mg. In this case, the content of $Ni(RuF_6)_2$ in the raw product was also calculated based on the mass of the starting Ru. The product was greenish, and it was poorly soluble in aHF.

Synthesis of $[Cu(XeF_2)_n](RuF_6)_2$ (n = 2, 4, 6)

The syntheses of Cu coordination compounds were carried out according to the general experimental procedure. The products were synthesized from $Cu(RuF_6)_2$ and XeF_2 in molar ratios of 1:2, 1:4, and 1:8 (excess XeF_2). The masses and amounts of reactants for each ratio are summarized in Table S2, Supporting Information. In all cases, the reddish-pink color of $Cu(RuF_6)_2$ changed to white within 5 minutes. The reactions in all cases lasted 24 h at room temperature. The product's isolation was carried out at temperatures lower than 273 K ($263\ K < T < 273\ K$). The products were poorly soluble in aHF.

Synthesis of $[Ni(XeF_2)_n](RuF_6)_2$ (n = 2, 6)

The synthesis and isolation procedure for the Ni compounds was the same as for the Cu coordination compounds. The reactions were carried out between $Ni(RuF_6)_2$ and XeF_2 in molar ratios of 1:2 and 1:12 (excess XeF_2). The masses and amounts of reactants for each ratio are summarized in Table S3, Supporting Information. The products were greenish, and they were poorly soluble in aHF.

Acknowledgements

The authors gratefully acknowledge the Slovenian Research and Innovation Agency (ARIS) for financial support of the Research Program P1–0045 (Inorganic Chemistry and Technology). Thanks also to Žan Zakošek for his assistance with data processing for the determination of the crystal structure of $[Cu(XeF_2)_6](RuF_6)_2$.

Conflict of Interest

The authors declare no conflicts of interest.

Data Availability Statement

The data that support the findings of this study are available from the corresponding author upon reasonable request.

Keywords: copper · nickel · ruthenate · xenon difluoride · X-ray diffraction

[1] N. Bartlett, *Proc. Chem. Soc.* **1962**, 218.
[2] K. O. Christe, *Chem. Commun.* **2013**, *49*, 4588.
[3] M. Tramšek, B. Žemva, *Acta Chim. Slov.* **2006**, *53*, 105.
[4] R. Hagiwara, F. Hollander, C. Maines, N. Bartlett, *Eur. J. Solid State Inorgan. Chem.* **1991**, *28*, 855.
[5] G. Tavčar, M. Tramšek, *J. Fluorine Chem.* **2015**, *174*, 14.
[6] Z. Mazej, E. Goreshnik, *Molecules* **2023**, *28*, 3370.
[7] G. Tavčar, E. Goreshnik, Z. Mazej, *J. Fluorine Chem.* **2006**, *127*, 1368.
[8] Z. Mazej, E. Goreshnik, *Inorg Chem.* **2008**, *47*, 4209.
[9] M. Tramšek, E. Goreshnik, G. Tavčar, *Zeitschrift Anorg. Allge. Chemie* **2022**, *648*, e202200301.
[10] E. Weise, W. Klemm, *Zeitschrift Anorg. Allge. Chemie* **1955**, *279*, 74.
[11] O. Graudejus, A. P. Wilkinson, L. C. Chacón, N. Bartlett, *Inorg. Chem.* **2000**, *39*, 2794.
[12] B. Koch, T. Graubner, A. J. Karttunen, F. Kraus, *Eur. J. Inorg. Chem.* **2025**, *28*, e202400767.
[13] G. Lucier, J. Muenzenberg, W. J. Casteel, N. Bartlett, *Inorg. Chem.* **1995**, *34*, 2692.
[14] T. Bunič, M. Tramšek, E. Goreshnik, B. Žemva, *Collect Czech Chem. Commun.* **2008**, *73*, 1645.
[15] Z. Mazej, in *Modern Synthesis Processes and Reactivity of Fluorinated Compounds* (Eds: H. Groult, F. Leroux, A. Tressaud), Elsevier, London **2017**, p. 587.
[16] L. Greb, *Chem. Eur. J.* **2018**, *24*, 17881.
[17] R. Craciun, R. T. Long, D. A. Dixon, K. O. Christe, *J. Phys. Chem. A* **2010**, *114*, 7571.
[18] G. Tavčar, M. Tramšek, T. Bunič, P. Benkič, B. Žemva, *J. Fluorine Chem.* **2004**, *125*, 1579.
[19] M. Tramšek, B. Žemva, *J. Fluorine Chem.* **2006**, *127*, 1275.
[20] Z. Mazej, E. Goreshnik, *Eur. J. Inorg. Chem.* **2023**, *26*, e202300046.
[21] D. Gantar, I. Leban, B. Frlec, J. H. Holloway, *J. Chem. Soc., Dalton Trans.* **1987**, 2379.
[22] P. Benkič, Z. Mazej, *Zeitschrift Anorg. Allg. Chem.* **2001**, *627*, 1952.
[23] Z. Mazej, E. Goreshnik, *Eur. J. Inorg. Chem.* **2022**, *2022*, e202101076.
[24] S. H. Elder, G. M. Lucier, F. J. Hollander, N. Bartlett, *J. Am. Chem. Soc.* **1997**, *119*, 1020.
[25] Z. Mazej, P. Benkič, A. Tressaud, B. Žemva, *Eur. J. Inorg. Chem.* **2004**, *2004*, 1827.
[26] B. G. Müller, *Angew. Chem.* **1987**, *99*, 685.
[27] M. A. Halcrow, *Dalton Trans.* **2003**, 4375.
[28] M. A. Halcrow, *Chem. Soc. Rev.* **2013**, *42*, 1784.
[29] J. Conradie, *Inorg. Chim. Acta* **2019**, *486*, 193.
[30] K. Nakamoto, *Infrared and Raman Spectra of Inorganic and Coordination Compounds. Part A: Theory and Applications in Inorganic Chemistry*, Wiley, Hoboken, NJ **2009**, pp. 221–229.
[31] Z. Mazej, E. Goreshnik, *Solid State Sci.* **2006**, *8*, 671.
[32] Z. Mazej, *J. Fluorine Chem.* **2004**, *125*, 1723.
[33] S. T. Breviglieri, É. T. G. Cavalheiro, G. O. Chierice, *Thermochim. Acta* **2000**, *356*, 79.
[34] A. Frontera, *Molecules* **2020**, *25*, 3419.
[35] S. Reichman, F. Schreiner, *J. Chem. Phys.* **1969**, *51*, 2355.
[36] H. S. A. Elliott, J. F. Lehmann, H. P. A. Mercier, H. D. B. Jenkins, G. J. Schrobilgen, *Inorg. Chem.* **2010**, *49*, 8504.
[37] M. Tramšek, P. Benkič, B. Žemva, *Inorg. Chem.* **2004**, *43*, 699.
[38] R. G. Pearson, *Inorg. Chem.* **1988**, *27*, 734.
[39] R. Zibaseresht, R. M. Hartshorn, *Acta Crystallogr. E Struct. Rep. Online* **2006**, *62*, i19.
[40] M. Tramšek, E. Goreshnik, G. Tavčar, *Acta chim. Slov.* **2016**, *63*, 369.
[41] G. Tavčar, B. Žemva, *Inorg. Chem.* **2013**, *52*, 4319.
[42] D. Peters, R. Miethchen, *J. Fluorine Chem.* **1996**, *79*, 161.
[43] Rigaku Oxford Diffraction, *CrysAlisPro Software System, Version 41_64.93a*, Rigaku Corporation, Oxford, UK **2018**.
[44] G. M. Sheldrick, *Acta Crystallogr. A Found Crystallogr.* **2008**, *64*, 112.
[45] G. M. Sheldrick, *Acta Crystallogr. C Struct. Chem.* **2015**, *71*, 3.
[46] L. J. Farrugia, *J. Appl. Crystallogr.* **2012**, *45*, 849.
[47] Diamond - Crystal and Molecular Structure Visualization, Crystal Impact - Dr. H. Putz & Dr. K. Brandenburg GbR, Kreuzherrenstr. 102, 53227 Bonn, Germany, https://www.crystalimpact.com/diamond/references.htm.
[48] Deposition numbers (https://www.ccdc.cam.ac.uk/services/structures?id=doi:10.1002/ejic.202500275) 2449880 (for $[Cu(XeF_2)_2](RuF_6)_2$), 2449881 (for $[Ni(XeF_2)_6](RuF_6)_2$), 2449882 (for $Cu(RuF_6)_2$), 2449883 (for $[Ni(XeF_2)_2](RuF_6)_2$) and 2449884 (for $[Cu(XeF2)_6](RuF_6)_2$) contain the supplementary crystallographic data for this paper. These data are provided free of charge by the joint Cambridge Crystallographic Data Centre and Fachinformationszentrum Karlsruhe Access Structures service.
[49] A. W. Jache, G. H. Cady, *J. Phys. Chem.* **1952**, *56*, 1106.

Manuscript received: May 28, 2025
Revised manuscript received: June 20, 2025
Version of record online: